

VALIDATION OF THE ONERA DAMAGE MODEL THROUGH COMPARISONS WITH MULTI-INSTRUMENTED STRUCTURAL TESTS ON INTERLOCK WOVEN CERAMIC MATRIX COMPOSITES

F. Laurin^{1*}, N. Tableau², M. Kaminski¹, Z. Aboura², F. Bouillon³

¹ONERA-The French Aerospace Lab, DMSC/MC², F-92322 Châtillon, France

²UTC-Université de Technologie de Compiègne, Laboratoire Roberval, F- 60205 Compiègne, France

³SAFRAN-HERAKLES, F-33187 Le Haillan, France

*frederic.laurin@onera.fr

Keywords: Ceramic matrix composites, Continuum damage modelling, Failure, Multi-instrumented tests.

Abstract

This paper presents the Onera damage model adapted to predict damage and failure mechanisms encountered in a new generation of interlock woven composite with ceramic matrix. The predictions of the present approach are compared successfully with different multi-instrumented tests performed at Onera or UTC in terms of non-linear behaviour, damage evolution and macroscopic stress at final failure.

1. Introduction

The present study deals with the damage and strength prediction of structures made of Ceramic Matrix Composites (CMCs). In the early 90's, some macroscopic damage approaches have been developed specifically for 2D woven CMC [1,2] and used tensorial damage variables assuming that the damage orientation is load-dependent. The formalism of such approaches seems well adapted to describe the damage mechanisms observed in CMCs but are very complex and thus difficult to transfer to aeronautical design offices. Therefore, an alternative damage approach, called the Onera Damage Model for Composites with Ceramic Matrix (ODM-CMC) has been developed at Onera and presents, in our opinion, an interesting trade-off between complexity of the modelling, accuracy of the predictions, and transferability to a design office. The ODM-CMC model has been initially proposed and validated for 2D woven CMC [3]. This paper presents (i) the enhanced Onera Damage Model in order to predict damage and failure of a new generation of interlock woven composites with ceramic matrix provided by Herakles and its validation through comparisons with multi-instrumented tests. In the section 2, the ODM-CMC approach is presented and the different modelling assumptions are discussed thanks to some multi-instrumented tests on composite structures performed at Onera or UTC. A special attention is paid for a robust implementation of this approach in order to obtain reasonable time of computation in a commercial finite element code. Finally, the comparisons between the predicted non-linear damageable behaviour and the available test results are presented in the section 3.

2. Presentation of the Onera damage model for composites with ceramic matrix

2.1. General presentation of the model

The Onera Damage Model for Composites with Ceramic Matrix is based on continuum damage approaches defined at the macroscopic scale, in order to be used in design office for the strength predictions of composite structures representative of some industrial problematic. For the considered new generation of interlock woven CMC, it is assumed that the observed non-linearities are only due to the damage and failure mechanisms. The present approach is thermodynamically consistent and thus the macroscopic behaviour, expressed in Eq. 1, derives directly from the Helmholtz free energy.

$$\underline{\underline{\sigma}} = \underline{\underline{C}}^{eff} : (\underline{\underline{\varepsilon}} - \underline{\underline{\varepsilon}}^{th} - \underline{\underline{\varepsilon}}^0) - \underline{\underline{C}}^0 : (\underline{\underline{\varepsilon}}^s + \underline{\underline{\varepsilon}}^r - \underline{\underline{\varepsilon}}^0) \quad \text{with} \quad \underline{\underline{C}}^{eff} = \left(\underline{\underline{S}}^0 + \sum_i d_i^m \underline{\underline{H}}_i^m + \sum_j d_j^f \underline{\underline{H}}_j^f \right)^{-1} \quad (1)$$

where $\underline{\underline{\sigma}}$ is the stress tensor, $\underline{\underline{C}}^{eff}$ is the effective elastic stiffness tensor taking into account the effects of the different damage and failure mechanisms, $\underline{\underline{C}}^0$ the initial elastic stiffness tensor, $\underline{\underline{\varepsilon}}$ the total strain tensor, and $\underline{\underline{\varepsilon}}^{th}$ the thermal strain tensor. In the present approach, the effects of damage mechanisms (yarn/matrix debondings, transverse cracking in the matrix ...) on the macroscopic behaviour are distinguished from those of fibre yarn failures which induce a sudden and huge decrease of the macroscopic rigidity. This point is considered in the ODM by increasing the initial elastic compliance $\underline{\underline{S}}^0$ with two terms describing the effects of matrix damages ($\sum d_i^m \underline{\underline{H}}_i^m$) and those of yarn failures ($\sum d_j^f \underline{\underline{H}}_j^f$). Finally, the $(\underline{\underline{\varepsilon}}^0, \underline{\underline{\varepsilon}}^s, \underline{\underline{\varepsilon}}^r)$ specific strain tensors are defined in the section 2.3.

2.2. Damage mechanisms

Contrary to composite with polymer matrix, composites with ceramic matrix present a low contrast between the different elementary constituents inducing that the orientation of damages is mostly load-dependent. In order to estimate the accuracy of such an assumption for new generation of woven interlock CMC, an off-axis incremental tensile test at 45°, on a specimen provided by Herakles, has been performed at UTC [4]. This test has been multi-instrumented with (i) acoustic emission in order to estimate the onset and the evolution of the matrix damages, (ii) digital images stereo-correlation in order to measure the strains (at mesoscopic scale and at the macroscopic scale thanks to large virtual strain gauges) and finally (iii) with SEM fractography in order to study the different damage mechanisms. SEM micrographs have been taken at different loading levels in order to study the evolution of the damages both on the upper face and on one free-edge of the specimen as illustrated in Figure 1. Thanks to the quality and the resolution of SEM images (the right picture reported in Figure 1 is constituted with 4000 SEM elementary pictures), it is possible to observe the different cracks at the free edges of the specimen. The observed cracks at the upper face are normal to the applied loading. Nevertheless, it is important to note that these observed cracks are located in a surface layer called the “seal-coat” which is due to the manufacturing process. Therefore, additional SEM micrographs have to be performed at mid-thickness of the specimen (*i.e.* within the sample, far from the edges) in order to demonstrate that the orientations of the damages in the material are load-dependent. Moreover, through the analysis of the SEM pictures taken on a free-edge of the specimen, it has been demonstrated

that yarn/matrix debondings occur even during tensile loading. These debondings are essentially due to some fibre yarn re-arrangements at the mesoscopic scale during the loading.

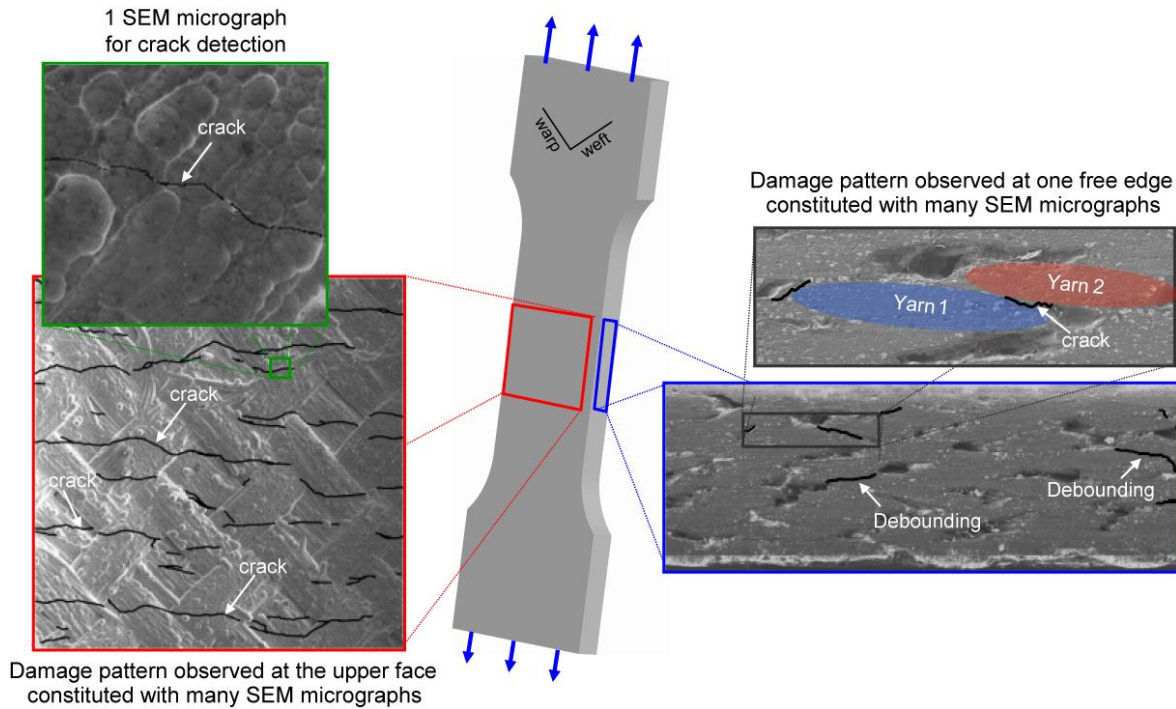


Figure 1. Observation of the damage pattern (matrix cracking and yarn/matrix debondings) in a specimen subjected to an off-axis tensile loading at 45° through SEM pictures.

Considering the different damage mechanisms, the ODM-CMC model is a thermo-dynamical damage model considering 5 matrix scalar damage variables, illustrated in Figure 2, which are (i) the damages in the weft direction noted d_1^m , (ii) the damages in the warp direction noted d_2^m (iii) the yarn/matrix debondings in the out-of-plane direction noted d_3^m , and the matrix damages oriented at 45° noted (iv) d_{45}^m and at 135° noted (v) d_{135}^m .

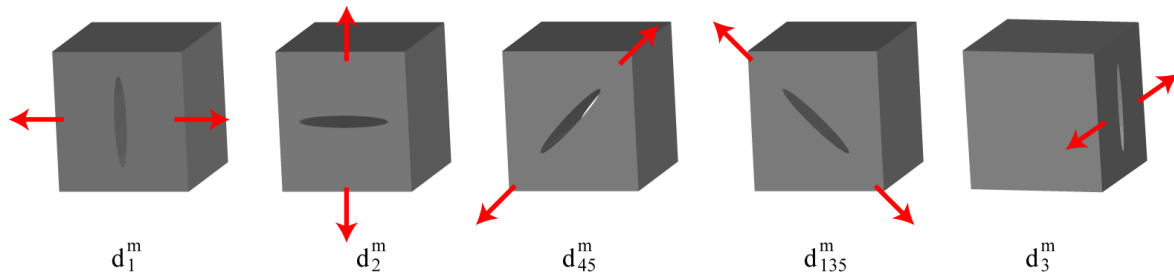


Figure 2. Presentation of the five matrix damage variables in the ODM-CMC model.

Nevertheless, the driving forces associated with the in-plane damage variables (see Eq. 3) have been formulated in order to obtain damage predictions which are equivalent to those obtained with a tensorial damage approach, such as [1,2], for off-axis tensile tests at 0°, 90°, 45° and 135°. Therefore, the analysis of FE simulations performed with the present approach on industrial test cases remains rather simple because of the use of simple scalar damage variables which present a clear physical meaning and thus should permit to transfer such an approach into a design office. The thermo-dynamical and driving forces associated to the different in-plane damage variables are expressed respectively in Eq. 2 and 3.

$$\begin{cases} z_1^m = \frac{1}{2} \left(\varepsilon_1^{d_1^{m+}} : C_{11}^0 : \varepsilon_1^{d_1^{m+}} + b_1 \varepsilon_6^{d_1^{m+}} : C_{66}^0 : \varepsilon_6^{d_1^{m+}} + b_2 \varepsilon_5^{d_1^{m+}} : C_{55}^0 : \varepsilon_5^{d_1^{m+}} \right) \\ z_2^m = \frac{1}{2} \left(\varepsilon_2^{d_2^{m+}} : C_{22}^0 : \varepsilon_2^{d_2^{m+}} + b_1 \varepsilon_6^{d_2^{m+}} : C_{66}^0 : \varepsilon_6^{d_2^{m+}} + b_2 \varepsilon_4^{d_2^{m+}} : C_{44}^0 : \varepsilon_4^{d_2^{m+}} \right) \\ z_6^m = \frac{1}{4} \left(\varepsilon_1^{d_1^{m+}} : C_{11}^0 : \varepsilon_6^{d_1^{m+}} + \varepsilon_2^{d_2^{m+}} : C_{22}^0 : \varepsilon_6^{d_2^{m+}} + b_1 \left(\varepsilon_6^{d_1^{m+}} : C_{66}^0 : \varepsilon_1^{d_1^{m+}} + \varepsilon_6^{d_2^{m+}} : C_{66}^0 : \varepsilon_2^{d_2^{m+}} \right) \right) \end{cases} \quad (2)$$

$$y_1^m = z_1^m - |z_6^m|, \quad y_2^m = z_2^m - |z_6^m|, \quad y_{45}^m = \langle z_6^m \rangle_+ \quad \text{and} \quad y_{135}^m = \langle -z_6^m \rangle_+ \quad (3)$$

where thermo-dynamical forces depend on (i) the different components of the initial elastic stiffness tensor, (ii) on the parameters (b_1, b_2) which are material coefficients and (iii) on the positive strain tensor. The positive strain tensor, associated to a thermo-dynamical force, corresponds to the positive part, as proposed by [5], of the total strain tensor where all the components are zeros except those inducing damages and reported in Eq. 2. The use of the positive strain tensor is an elegant way to capture the reinforcement of the apparent onset of damage for combined compressive and shear loading, as demonstrated experimentally on former generation of 2D woven CMC [2], without introducing additional coefficients. The $\langle \cdot \rangle_+$ corresponds to the classical Macauley brackets.

On the considered interlock woven CMC, as illustrated in Figure 1, some yarn/matrix deboundings are observed for tensile loading while the total out-of-plane strain is negative due to Poisson effects. In order to introduce in the present macroscopic approach, these deboundings observed in tension due to yarn re-arrangements at the mesoscopic scale, the thermo-dynamical force z_3^{m+} has been introduced in the driving force y_3^m associated to the out-of-plane damage as reported in Eq. 4.

$$\begin{cases} z_3^m = \frac{1}{2} \left(\varepsilon_3^{d_3^{m+}} : C_{33}^0 : \varepsilon_3^{d_3^{m+}} + b_2 \varepsilon_4^{d_3^{m+}} : C_{44}^0 : \varepsilon_4^{d_3^{m+}} + b_2 \varepsilon_5^{d_3^{m+}} : C_{55}^0 : \varepsilon_5^{d_3^{m+}} \right) \\ z_3^{m+} = \frac{1}{2} \left(\alpha_1^+ \langle \varepsilon_1 \rangle_+ : C_{11}^0 : \langle \varepsilon_1 \rangle_+ + \alpha_2^+ \langle \varepsilon_2 \rangle_+ : C_{22}^0 : \langle \varepsilon_2 \rangle_+ + \alpha_6^+ \varepsilon_6 : C_{66}^0 : \varepsilon_6 \right) \end{cases} \quad (4)$$

with $y_3^m = z_3^m + z_3^{m+}$

where ($\alpha_1^+, \alpha_2^+, \alpha_6^+$) are material parameters which permits to calibrate the onset of out-of-plane damage during in-plane tensile tests. It can be noted that, for compressive loading, the deboundings are naturally predicted thanks to Poisson effects.

Finally, the evolution laws of the five damage variables are expressed in Eq. 5, where the parameter $y_{0_i}^m$ corresponds to the onset of damage, $d_{c_i}^m$ to the saturation of the damage which is currently observed for CMCs, and ($y_{c_i}^m, p_i^m$) are parameters which are linked to the damage evolution laws. It can be noted that the damages can only growth in order to ensure the second principle of thermodynamics.

$$d_i^m = d_{c_i}^m \left(1 - \exp \left(- \left(\frac{\langle \sqrt{y_i^m} - \sqrt{y_{0_i}^m} \rangle_+}{\sqrt{y_{c_i}^m}} \right)^{p_i^m} \right) \right) \quad \text{with} \quad \dot{d}_i^m \geq 0 \quad \text{and} \quad i = \{1, 2, 3, 4, 5, 135\} \quad (5)$$

2.3. Unilateral aspect of damage and residual strains

The present section is dedicated to the effect of the different damages and especially to the necessity to take into account the unilateral aspect of damage as illustrated in Figure 3, which presents the experimental behaviour of the studied new generation of CMC subjected to tensile/compressive loading in the weft direction. This test has been performed at Onera and has been multi-instrumented with DIC, extensometer and acoustic emission.

After generating matrix damages during the tensile loading, a low compressive loading is applied to the sample in order to observe the progressive recovery of the initial elastic Young modulus. The progressive closure of the cracks, inducing the evolution of the apparent elastic modulus for low compressive stress, is mainly due to the scattering on the orientation of the cracks in the material. Moreover, an important residual strain is observed after unloading at null stress, which is assumed to be due to the friction on the tips of the cracks and due to the relaxation of the thermal residual stresses in the elementary constituents induced during the manufacturing process.

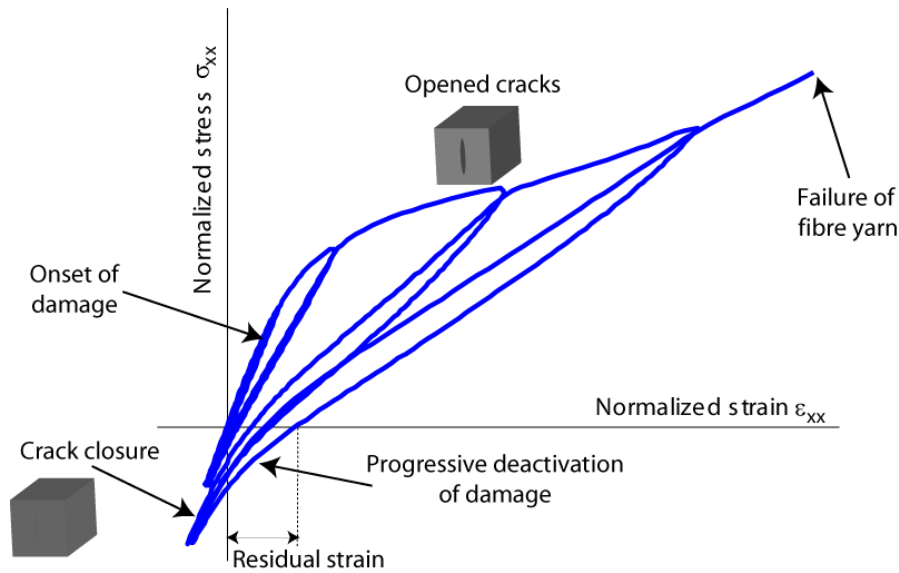


Figure 3. Experimental stress / strain curve of a new generation of CMC subjected to tensile/compressive loading in the weft direction and illustration of some key phenomena.

In order to describe the progressive deactivation of damages observed in Figure 3 for a tension/compression test in the weft direction, the effect tensor $\underline{\underline{H}}_1^m$ associated to the damage variable d_1^m is defined as a function of a progressive deactivation index (η_1) and of an effect tensor ($\underline{\underline{H}}_1^{m+}$) describing the effects of an open crack on the effective elastic stiffness, as reported in Eq. 6. The parameters ($h_{11}^{m+}, h_{55}^{m+}, h_{66}^{m+}$) are material coefficients. The cracks are assumed closed when the effective strain ($\underline{\underline{\varepsilon}}^d$) is inferior to $\varepsilon_1^0 - \Delta\varepsilon_1^{close}$ and opened when this strain is superior to $\varepsilon_1^0 + \Delta\varepsilon_1^{close}$. The progressive deactivation index evolves from 0 to 1 between these two bounds. The parameters ($\underline{\underline{\varepsilon}}^0, \Delta\varepsilon_i^{close}$) are material coefficients. The effect tensors and the associated deactivation indexes for the other damage variables can be obtained thanks to permutation of the indices.

$$\begin{aligned}
 \underline{\underline{H}}_1^m = \eta_1 \underline{\underline{H}}_1^{m+} \quad \text{with} \quad \eta_1 = \begin{cases} 1 & \text{if } \Delta \varepsilon_1^{close} \leq \varepsilon_1^d \\ \frac{1}{2} \left(1 - \cos \left(\frac{\pi}{2} \frac{\varepsilon_1^d + \Delta \varepsilon_1^{close}}{\Delta \varepsilon_1^{close}} \right) \right) & \text{if } -\Delta \varepsilon_1^{close} \leq \varepsilon_1^d \leq \Delta \varepsilon_1^{close} \\ 0 & \text{if } \varepsilon_1^d \leq -\Delta \varepsilon_1^{close} \end{cases} \\
 \text{with } \underline{\underline{H}}_1^{m+} = \begin{pmatrix} h_{11}^{m+} S_{11}^0 & 0 & 0 & 0 & 0 & 0 \\ & 0 & 0 & 0 & 0 & 0 \\ & & 0 & 0 & 0 & 0 \\ & & & 0 & 0 & 0 \\ \text{sym.} & & & h_{55}^{m+} S_{55}^0 & 0 & 0 \\ & & & & h_{66}^{m+} S_{66}^0 & 0 \end{pmatrix} \quad \text{and} \quad \underline{\underline{\varepsilon}}^d = \underline{\underline{\varepsilon}} - \underline{\underline{\varepsilon}}^{th} - \underline{\underline{\varepsilon}}^0
 \end{aligned} \tag{6}$$

Moreover, it is assumed that when a crack is closed, all the components of the elastic stiffness are restored, as reported in Eq. 6, even for the shear components. This point has been experimentally demonstrated for former generations of 2D woven CMC [6]. Ensuring the continuity of the mechanical response for complex multiaxial loadings while taking into account the unilateral aspect of damage is non-trivial. In order to fulfil this objective, a stored strain ($\underline{\underline{\varepsilon}}_s$) has been introduced in the proposed modelling. By assuming that the behaviour defined in Eq. 1 is continuous, even when the cracks evolve from an opened state to a closed one, the formulation of the stored strain rate is necessary defined as

$$\dot{\underline{\underline{\varepsilon}}}_s = -\underline{\underline{S}}_0 \sum_i \dot{\eta}_i d_i \underline{\underline{C}}^{eff} : \underline{\underline{H}}_i^{m+} : \underline{\underline{C}}^{eff} : (\underline{\underline{\varepsilon}} - \underline{\underline{\varepsilon}}^{th} - \underline{\underline{\varepsilon}}^0) \tag{7}$$

A special attention has been paid to the resolution of such a differential equation. In order to compute the increment of the stored strain, the integral of Eq. 7 is approximated with a 3th order Gaussian quadrature. This numerical solving method, contrary to a classical Euler method, permits to obtain solutions which are almost insensitive to the size of the increment, which is necessary to implement the proposed approach, in an efficient way, in an implicit FE code.

Finally, a residual strain ($\underline{\underline{\varepsilon}}_r$) has been introduced into the present model to describe accurately the available stress/strain curves. This residual strain is defined as a function of the evolution of the damage variables and its formulation, reported in Eq. 8, is rather consistent with the ones proposed for the stored strain (see Eq. 7).

$$\dot{\underline{\underline{\varepsilon}}}_r = \underline{\underline{S}}_0 \sum_i \chi_i \dot{d}_i \underline{\underline{C}}^{eff} : \underline{\underline{H}}_i^m : \underline{\underline{C}}^{eff} : (\underline{\underline{\varepsilon}} - \underline{\underline{\varepsilon}}^{th} - \underline{\underline{\varepsilon}}^0) \tag{8}$$

where the χ_i parameters are material coefficients which have to be identified. The integral of this differential equation is also solved with a 3th order Gaussian quadrature for the reasons previously mentioned.

2.4. Failure mechanisms

The rupture of the tested specimens is due to the failure of the fibre yarns. The failure patterns observed on off-axis tensile tests at 0° or 45° are illustrated in Figure 4. Contrary to the damage mechanisms, the failure patterns are clearly oriented by the microstructure of the material.

Considering the different failure mechanisms, the ODM-CMC model is a damage and failure approach considering also 4 scalar failure variables which are the yarn failure due to tensile loading in the weft and warp directions noted respectively d_1^{f+} and d_2^{f+} , and the yarn failure due to compressive loading in the weft and warp directions noted respectively d_1^{f-} and d_2^{f-} . The four driving forces and the associated failure variables are defined respectively in Eq. 9 and 10.

$$y_j^{f+} = \frac{1}{2} \langle \varepsilon_j \rangle_+ : C_{jj}^0 : \langle \varepsilon_j \rangle_+ \quad \text{and} \quad y_j^{f-} = \frac{1}{2} \langle -\varepsilon_j \rangle_+ : C_{jj}^0 : \langle -\varepsilon_j \rangle_+ \quad (9)$$

$$d_j^{f\pm} = \left(\frac{\langle \sqrt{y_j^{f\pm}} - \sqrt{y_{0_j}^{f\pm}} \rangle_+}{\sqrt{y_{c_j}^{f\pm}}} \right)^{p_j^{f\pm}} \quad \text{with} \quad d_j^{f\pm} \geq 0 \quad \text{and} \quad j = \{1, 2\} \quad (10)$$

where the parameter $y_{0_j}^{f\pm}$ corresponds to the onsets of yarn failure (equivalent to the failure of unnotched samples) in tension (noted with the index +) and in compression (noted with index -) and $(y_{c_j}^{f\pm}, p_j^{f\pm})$ are parameters which are linked to the progressive degradation laws.

The effect tensors $\underline{\underline{H}}_j^f$ associated with the failure of the fibre yarns are similar to those defined in Eq. 6. Nevertheless, the progressive degradation laws used for yarn failure are sudden and most of the time catastrophic for the material and induce softening behaviour as illustrated in Figure 4. The description of the softening behaviour due to yarn failures is necessary in order to predict accurately the final failure of composite structures containing geometrical singularities such as open-hole plates.

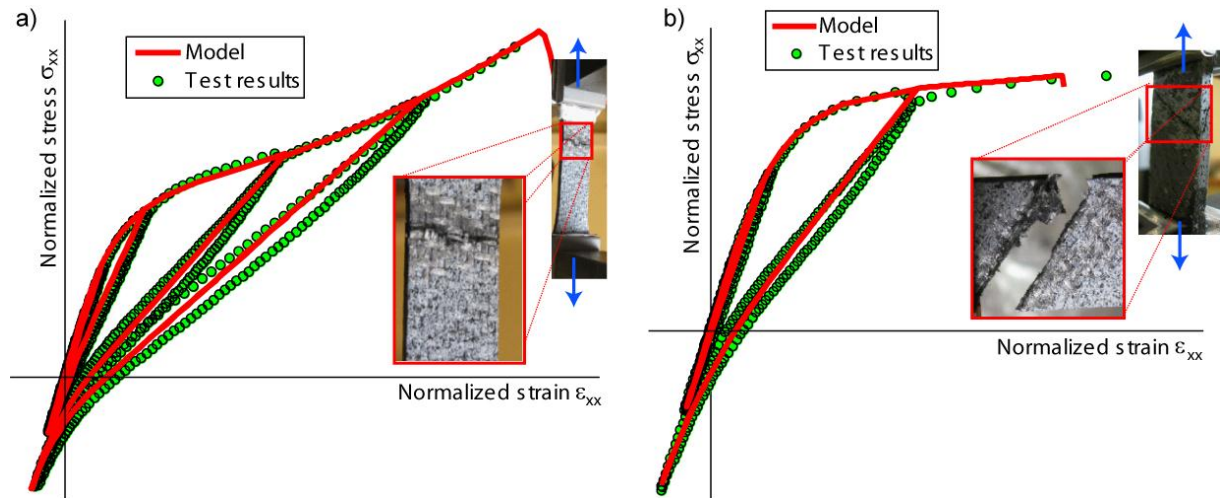


Figure 4. Comparison between the experimental strain/stress curves and the predictions obtained with ODM-CMC for a) an off-axis tensile test at 0° and b) an off-axis tensile tests at 45°.

3. Comparison with test results

Off-axis tension / compression tests at 0°, 90° and 45° on woven interlock CMC have been performed at Onera [7] with the multi-instrumentation presented previously. Each configuration of test has been repeated three times in order to estimate the scattering. The comparisons between the predicted stress/strain curves and the experimental data are in good agreement for the three considered directions in terms of non-linear behaviour, damage evolution and macroscopic stress at failure. Only the comparisons performed on off-axis tests at 0° and 45° are illustrated in Figure 4. Moreover, the unilateral aspect of damage is accurately described by the proposed modelling on the tested configurations.

4. Conclusions / Perspectives

The Onera Damage Model for Composites with Ceramic Matrix (ODM-CMC) has been adapted successfully to a new generation of woven interlock CMC. The different assumptions of the proposed approach have been validated thanks to multi-instrumented tests performed at Onera or UTC. This approach is currently implemented in the commercial finite element code Abaqus/standard in order to predict the strength of structures which are representative of industrial problematic.

Acknowledgements

The collaboration with Herakles is gratefully acknowledged. This work was supported under the PRC Composites, French research project funded by DGAC, involving SAFRAN Group, ONERA, and CNRS.

References

- [1] P. Ladevèze, A. Gasser, O. Allix. Damage mechanisms modeling for ceramic composites. *J. Engng Mater. Technol.*, Vol. 116(4): 331-336, 1994.
- [2] J.- F. Maire, P.-M. Lesne, R. Girard. An explicit behavioural damage model for the design of components in ceramic matrix composites. *Composites Science and Technology*, Vol. 58: 113-118, 1998.
- [3] L. Marcin, J. Maire, N. Carrère, E. Martin. Development of a macroscopic damage model for woven ceramic–matrix composites. *International Journal of Damage Mechanics*, Vol. 20:939-957, 2011.
- [4] N. Tableau, Z. Aboura, K. Khellil, L. Marcin, F. Bouillon. Intra and inter laminar characterization of a CMC composite material, In : *18^{ème} Journées Nationales des Composites, Nantes, France*, 12-14 June 2013.
- [5] J. Ju. On energy-based coupled elastoplastic damage theories: constitutive modeling and computational aspects. *Int J Solids Struct*, Vol 25:803–833, 1989.
- [6] J.- F. Maire, D. Paçou. Essais de traction-compression-torsion sur tubes composites céramiques, In : *10^{ème} Journées Nationales des Composites, Paris, France*, 29-31 October, 1996.
- [7] E. Hémon. Modèles multi-niveaux de prévision des durées de vie en fatigue des structures composites à matrice céramique pour un usage en turbomachines aéronautiques, *Doctorate thesis of University of Bordeaux I, France*, 2013.